

## Equivalent uniform dose and normal tissue complication probability of acute esophagitis in head-and-neck radiotherapy: Sensitivity to dose calculation accuracy

M.A. Mosleh-Shirazi<sup>1,2</sup>, A. Sheikholeslami<sup>3\*</sup>, E. Fathipour<sup>3</sup>,  
M. Mohammadianpanah<sup>2</sup>, M. Ansari<sup>2\*</sup>, S. Karbasi<sup>2</sup>, S.H. Hamed<sup>2</sup>,  
N. Khanjani<sup>2</sup>, M.R. Sasani<sup>4,5</sup>, P. Jafari<sup>6</sup>, R. Fardid<sup>1,3</sup>

<sup>1</sup>*Ionizing and Non-ionizing Radiation Protection Research Center, School of Paramedical Sciences, Shiraz University of Medical Sciences, Shiraz, Iran*

<sup>2</sup>*Department of Radio-oncology, Shiraz University of Medical Sciences, Shiraz, Iran*

<sup>3</sup>*Department of Radiology and Radiobiology, School of Paramedical Sciences, Shiraz University of Medical Sciences, Shiraz, Iran*

<sup>4</sup>*Medical Imaging Research Center, Shiraz University of Medical Sciences, Shiraz, Iran*

<sup>5</sup>*Department of Radiology, School of Medicine, Shiraz University of Medical Sciences, Shiraz, Iran*

<sup>6</sup>*Department of Biostatistics, School of Medicine, Shiraz University of Medical Sciences, Shiraz, Iran*

### ABSTRACT

#### ► Original article

##### \*Corresponding authors:

Mansour Ansari, M.D.,

E-mail: [maansari@sums.ac.ir](mailto:maansari@sums.ac.ir)

Arefeh Sheikholeslami, M.Sc.

E-mail:

[arefeh.1373@yahoo.com](mailto:arefeh.1373@yahoo.com)

Received: December 2020

Final revised: June 2021

Accepted: July 2021

*Int. J. Radiat. Res., April 2022;*  
20(2): 447-454

DOI: 10.52547/ijrr.20.2.28

**Keywords:** Dose calculation model, NTCP, EUD, Head-and-neck cancer.

**Background:** To quantify the influence of photon dose-calculation algorithm selection on the cervical esophagus (CE) dose indices and the derived equivalent uniform dose (EUD) and normal-tissue complication probability (NTCP) for acute esophagitis in patients with head-and-neck cancer (HNC). **Materials and Methods:** The Fast Photon Effective Path (FPEP) and Collapsed-Cone Convolution Superposition (CCCS) algorithms on the Prowess Panther treatment planning system were compared for 30 patients (six tumor sites). The Lyman-Kutcher-Burmann (LKB) model was used to calculate the EUDs and NTCPs. **Results:** On average, the more simplistic FPEP algorithm overestimated the mean dose to CE planning organ-at-risk volumes (PRVs) by 2.0% ( $p = 0.003$ ). The average absolute difference in mean dose was 2.7% and the maximum difference was 9.3%. The  $V_{5Gy}$ ,  $V_{10Gy}$ ,  $V_{15Gy}$ ,  $V_{20Gy}$ ,  $V_{25Gy}$  and  $V_{30Gy}$  values were significantly higher with FPEP, while the point-dose and  $D_{2cc}$  hot spots were similar. In turn, the dose differences led to an underestimation of the LKB-model prediction of the EUD by 1.4% ( $p = 0.297$ ). The mean absolute difference in EUD was 4.5% and the maximum difference was 15.3%. In the 14-50 Gy mean dose range, the resulting NTCPs with FPEP were lower on average by 2.6% than CCCS ( $p = 0.041$ ). **Conclusions:** In the group of HNC patients considered in this study, the EUD and NTCP for acute esophagitis showed to be moderately sensitive to the choice of dose-calculation algorithm. Despite an overestimated mean dose by the simpler algorithm, the NTCP underestimation, which can be large in some patients, is of clinical concern.

### INTRODUCTION

Radiation therapy (RT) treatment planning systems (TPSs) normally offer more than one dose calculation algorithm. To achieve reliable results in RT treatment planning, the dose distribution should be obtained by using the most accurate algorithms available in TPSs (<sup>1,2</sup>).

There are several radiobiological models that attempt to predict a tumor control probability, as well as normal tissue complication probabilities (NTCPs) for a variety of relevant clinical endpoints. These models, in addition to optimizing and evaluating treatment plans and quantifying the probabilities of local control and normal tissue side effects, may be used in evaluation of the effects of

dose uncertainty and patient position on treatment outcome (<sup>3</sup>). For example, head-and-neck squamous cell carcinomas (SCCs) are known to be radiobiologically sensitive to changes in factors such as dose, time and fractionation (<sup>4,5</sup>).

Normal tissue effects play an important role in decision making in the optimization of treatment plans. This becomes more critical by the fact that in many clinical situations, organ-at-risk (OAR) doses have to approach their tolerance limits.

Employing different dose calculation algorithms lead to different dose-volume histograms (DVHs) (<sup>6-10</sup>). Thus, as the DVH is one of the key inputs to an NTCP model, different NTCPs will be produced by the models when different dose calculation algorithms are used (<sup>1,2</sup>). The accuracy of these dose calculation

algorithms can, therefore, be critical <sup>(11)</sup>. Many studies have evaluated the accuracy of different dose calculation algorithms for a wide range of different parameters and circumstances and have found various magnitudes of differences in the calculated dose depending on the algorithms and the extent and types of tissue heterogeneities and contour irregularities <sup>(12-22)</sup>.

Radiobiological dose-response relationships are usually nonlinear <sup>(23)</sup>. In cases where there is a steep gradient in the relationship between NTCP and dose, the response of the organ is sensitive to dose variations and small changes in dose can be amplified into larger differences in NTCP <sup>(10, 24)</sup>. In contrast, a low gradient would mean that the NTCP is relatively insensitive to changes in dose and, consequently, to the choice of dose calculation algorithm.

The impact of employing different dose calculation algorithms on NTCP of some OARs have been studied, the findings of which are quite varied <sup>(1, 2, 11, 12, 15, 24-30)</sup>. These variations can be due to differences in the nature of the effects of complex anatomy on the dose to OARs calculated by different classes of algorithms, as well as individual patient OAR DVHs, the magnitude of the corresponding equivalent uniform dose (EUD) and where it may fall on the EUD-NTCP curve, and the shape and steepness of that relationship. The situation for each type of OAR that is of interest requires its own investigation, as there seems to be no general rule.

Swallowing dysfunction is an important side effect of RT for head-and-neck cancer (HNC) and esophagitis is one of its main causes. This normal-tissue effect has a profound effect on patients' quality of life and can even have a negative impact on their life expectancy <sup>(31)</sup>.

The head-and-neck region, due to the wide heterogeneity of different soft tissues, air cavities, bones, etc. and the relative complexities of its internal and external contours, poses a challenge for accurate dose calculation <sup>(32)</sup>. Moreover, RT is a highly-established and key treatment modality for HNC and a very large number of patients worldwide undergo RT with curative intent <sup>(5)</sup>. Further, patient-related issues, such as acute side effects, can be among the most common causes of interruptions during a course of RT for head-and-neck SCC <sup>(33)</sup>. Despite these facts, only a few studies have been published regarding the influence of dose calculation algorithms on the NTCP of OARs in head-and-neck RT <sup>(29, 34)</sup>. In particular, to the best of our knowledge, no published paper has assessed this effect for the cervical (upper) esophagus as an OAR for acute esophagitis.

Since the accuracy of a dose calculation algorithm affects the results of NTCP models, and the magnitude of the effects depend on the specific site and organs of interest, the influence of calculation algorithms merit further investigation, especially in a

site-specific manner. To that end, the purpose of this study was to compare two photon dose calculation algorithms and their respective effects on physical dose indices and the consequent radiobiological quantities of EUD and NTCP of the cervical esophagus (CE) for acute esophagitis in patients with HNC. To the best of our knowledge, such an investigation has not been published to date. The choice of this OAR reflects our research group's interest in its dose-response relationship and its role in swallowing dysfunction, given the detrimental effects of this normal-tissue effect on patients. We compared an example each of a simple and an advanced dose calculation algorithm used in a commercial TPS. To gain some insight into the processes involved, given the complex geometry of the head and neck, we limited the investigation to the effects of tissue inhomogeneities and contour irregularities and, therefore, considered 3D conformal treatment plans in this study. However, the findings can also be useful to some extent in treatment planning of various types of IMRT in which faster calculations are used during optimizations based on radiobiological quantities such as EUD and NTCP.

## MATERIALS AND METHODS

### Treatment planning

We chose a relatively simple, effective-pathlength-type calculation algorithm, used in the TPS for interim, fast calculations during intensity-modulated radiation therapy (IMRT) optimization. The other selected algorithm was an established, full-scatter, convolution-superposition-type one used widely for clinical 3D conformal plans as well as in accurate, final calculations in IMRT optimization.

The treatment plans of 30 patients with HNC were used in this study (table 1). All of the patients had been previously planned and treated at Namazi Teaching Hospital, Shiraz University of Medical Sciences with 3D conformal RT. The prescribed doses were 36 to 70 Gy, 2 Gy per fraction, 5 fractions per week. This study was approved by the Research Ethics Committee of Shiraz University of Medical Sciences (certificate number: IR.SUMS.REC.1398.130; approval date: 20/02/2019).

The patients had been scanned in the head-and-neck region and computed tomography images with slice thickness of 2.5 mm were available. The TPS used was Prowess Panther (Concord, CA, USA) (version 5.4). The 6 MV beam data for the same Elekta linear accelerator (Crawley, UK) was used in all plans. For the purposes of this study, the CE was contoured separately, from 1 cm below the inferior edge of the cricoid cartilage to the sternal notch <sup>(35)</sup>. Each contour was individually approved by a specialist radiologist. It was then grown by a 3 mm,

3D margin to produce the corresponding planning organ-at-risk volume (PRV). The number of patient treatment phases varied from 1 to 3 phases, and 2 to

4 treatment beams from cardinal gantry directions (or within 15° of them) were used in each phase (table 1).

**Table 1.** Summary of the patients' demographic information.

| Tumor Site   | No. of patients (%) | Sex          | Mean age | T stage              | No. of phases | No. of beams per phase | Beam angles |          |     |      |            |
|--------------|---------------------|--------------|----------|----------------------|---------------|------------------------|-------------|----------|-----|------|------------|
|              |                     |              |          |                      |               |                        | 0°          | 75° -85° | 90° | 180° | 270° -285° |
| Larynx       | 8 (27)              | F: 1<br>M: 7 | 55.3     | T1-T2: 4<br>T3-T4: 4 | 1-3           | 2-3                    | 4           | 6        | 7   | 0    | 9          |
| Supraglottis | 6 (20)              | F: 0<br>M: 6 | 62.7     | T1-T2: 3<br>T3-T4: 3 | 1-3           | 2-3                    | 6           | 4        | 12  | 0    | 14         |
| Glottis      | 4 (13)              | F: 1<br>M: 3 | 67.3     | T1-T2: 1<br>T3-T4: 3 | 1             | 2                      | 0           | 2        | 1   | 0    | 4          |
| Nasopharynx  | 7 (23)              | F: 1<br>M: 6 | 55.7     | T1-T2: 3<br>T3-T4: 4 | 1-3           | 3-4                    | 12          | 2        | 15  | 1    | 17         |
| Oropharynx   | 3 (10)              | F: 0<br>M: 3 | 55.7     | T1-T2: 2<br>T3-T4: 1 | 2-3           | 2-3                    | 6           | 0        | 7   | 0    | 7          |
| Hypopharynx  | 2 (7)               | F: 0<br>M: 2 | 59.5     | T1-T2: 2             | 1-3           | 2-3                    | 3           | 0        | 4   | 0    | 3          |

The Prowess Panther TPS offers two classes of photon dose calculation algorithms, namely, *conventional* and *convolution* models. The conventional model uses measured data to perform calculations. The simplest model is called *Fast Photon*, which assumes unit density throughout the medium. The second conventional algorithm is called *Fast Photon Effective Path Length* (FPEP). The FPEP model, is a relatively simple algorithm based on data measured in a water phantom, but it takes into account the effect of primary photons passing through heterogeneous tissues by calculating an effective pathlength through the media. In contrast, the convolution method first fits a model to the data and then uses the model to perform calculations. The *Collapsed Cone Convolution Superposition* (CCCS) algorithm is a full 3D dose calculation model that performs full heterogeneity calculations for primary and scattered radiation<sup>(36)</sup>. The convolution-superposition type of algorithm is widely used in many TPSs and is considered as one of the most accurate analytical models of dose calculation in RT<sup>(32)</sup>. We compared the FPEP and CCCS algorithms in this study.

### Radiobiological modeling

The Lyman-Kutcher-Burmann (LKB) model<sup>(37,38)</sup> in the BioSuite software<sup>(39)</sup> was used to calculate the EUDs and NTCPs. The LKB model is well-established in NTCP calculation<sup>(31, 40-42)</sup>. BioSuite is a reliable software that has found increasing use in NTCP modeling studies<sup>(43-46)</sup>.

The DVHs of the CE PRVs were entered into BioSuite and the EUD and NTCP of acute esophagitis was calculated for each patient. The selected parameters of the LKB model were obtained from the study of Belderbos *et al.*<sup>(41)</sup> as follows:  $m$  (slope) = 0.36,  $TD_{50}$  (tolerance dose for 50% complication rate of the normal organ) = 47 Gy,  $n$  (volume effect parameter) = 0.069. An alpha/beta value of 10 Gy was also used<sup>(47, 48)</sup>.

Finally, to test the sensitivity of various published LKB model parameters for the NTCP of esophagitis on differences in dose calculation of the CE PRV DVHs, we selected one typical patient from each tumor site and calculated their NTCPs using three other sets of LKB model parameters. The models parameters were given by Chapet *et al.*<sup>(42)</sup> ( $TD_{50}$  = 51 Gy,  $m$  = 0.32,  $n$  > 4.88), Zhue *et al.*<sup>(31)</sup> ( $TD_{50}$  = 46 Gy,  $m$  = 0.15,  $n$  > 4.88) and Nijkam *et al.*<sup>(40)</sup> ( $TD_{50}$  = 50.4 Gy,  $m$  = 0.25,  $n$  = 0.13).

We employed the Wilcoxon test for statistical analysis using the IBM SPSS software (version 16). A  $p$ -value < 0.05 was considered statistically significant.

## RESULTS

### Calculated dose

Figure 1 shows typical cumulative DVHs of the CE PRV in four examples of the studied tumor types for both dose calculation algorithms. The results of the effects of the two algorithms on the DVH of the CE PRV, stated in detail as  $V_{1Gy}$  to  $V_{70Gy}$  averaged over all patients, are shown in table 2.

Averaged over all patients, the CE PRV mean doses calculated with the FPEP and CCCS algorithms were 18.6 Gy and 18.2 Gy, respectively ( $p$  = 0.003). The differences (FPEP- CCCS) between the CE PRV mean doses calculated by the two algorithms in individual patients ranged from -0.8 Gy to 1.7 Gy. The average absolute difference between the CE PRV mean doses from the two calculation algorithms was 0.5 Gy.

As for the hot spots, the mean doses of the hottest two cubic centimeters ( $D_{2cc}$ ) of the CE PRV calculated with the two algorithms were 29.8 Gy and 30.1 Gy, respectively. The average of the maximum point doses of this structure in the two algorithms were both 38.2 Gy. The differences in  $D_{2cc}$  and maximum dose point were, however, not statistically significant ( $p$  = 0.688 and 0.750, respectively).

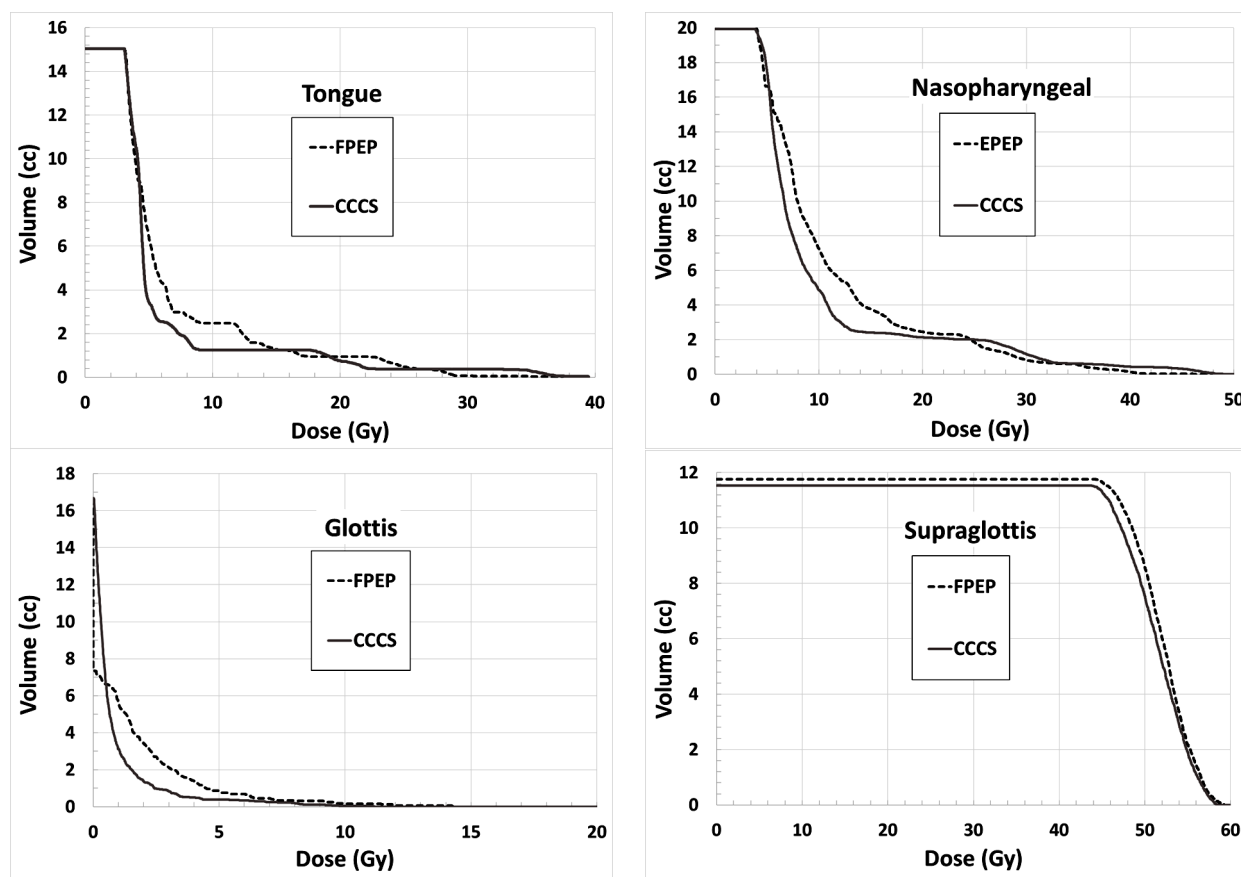


**Figure 1.** Cumulative DVHs of the CE PRVs in four typical patients with different tumor sites, calculated using the CCCS and FPEP algorithms.

**Table 2.** Means and standard deviations of several  $V_x$  values of the patients' CE PRVs as calculated by the two algorithms (\* denotes  $p < 0.05$ ).

| $V_x$ | $V_{1Gy}$<br>(%) | $V_{5Gy}$<br>(%) | $V_{10Gy}$<br>(%) | $V_{15Gy}$<br>(%) | $V_{20Gy}$<br>(%) | $V_{25Gy}$<br>(%) | $V_{30Gy}$<br>(%) | $V_{35Gy}$<br>(%) | $V_{40Gy}$<br>(%) | $V_{45Gy}$<br>(%) | $V_{50Gy}$<br>(%) | $V_{55Gy}$<br>(%) | $V_{60Gy}$<br>(%) | $V_{65Gy}$<br>(%) | $V_{70Gy}$<br>(%) |
|-------|------------------|------------------|-------------------|-------------------|-------------------|-------------------|-------------------|-------------------|-------------------|-------------------|-------------------|-------------------|-------------------|-------------------|-------------------|
| CCCS  | 54.2 ± 19.9      | 37.6 ± 27.8      | 27.1 ± 26.2       | 25.1 ± 26.3       | 24.8 ± 26.9       | 23.8 ± 26.5       | 23.4 ± 26.5       | 22.9 ± 26.6       | 22.6 ± 26.6       | 21.9 ± 26.4       | 21.3 ± 26.1       | 20.2 ± 25.5       | 19.3 ± 25.0       | 16.1 ± 22.3       | 12.1 ± 17.4       |
| FPEP  | 52.1 ± 22.1      | 41.7 ± 29.5      | 30.4 ± 27.0       | 26.5 ± 26.3       | 25.0 ± 26.4       | 24.2 ± 26.5       | 23.7 ± 26.6       | 23.0 ± 26.6       | 22.5 ± 26.7       | 21.9 ± 26.8       | 20.8 ± 26.8       | 20.5 ± 26.4       | 19.0 ± 25.5       | 16.2 ± 24.2       | 13.1 ± 20.8       |
| Diff. | -2.1             | +4.1*            | +3.3*             | +1.4*             | +0.2*             | +0.4*             | +0.3*             | +0.1              | -0.1              | 0.0               | -0.5              | +0.3              | -0.3              | +0.1              | +1.0              |

### Calculated EUD and NTCP

Averaged over all patients, the EUDs resulting from the DVHs calculated by the FPEP and CCCS algorithms were 28.4 Gy and 28.7 Gy, respectively. Figure 2 Shows the NTCP values for the EUDs derived from individual DVHs calculated by both algorithms for each patient. The horizontal axis values are the EUDs from the CCCS algorithm.

Figure 3 shows the corresponding differences between the EUDs obtained from the two algorithms (FPEP- CCCS). The differences in individual patients ranged from -4.4 Gy to +2.0 Gy. On average, the FPEP algorithm underestimated EUDs by 0.4 Gy, although not statistically significant ( $p = 0.297$ ). The mean absolute difference over all patients was 1.3 Gy.

The CE PRV NTCPs of all 30 patients predicted by the LKB model from the DVHs calculated using the CCCS and FPEP algorithms are plotted in figure 4 against the CCCS-calculated mean dose to the CE PRV.

The corresponding differences between the NTCPs obtained from the two algorithms are shown in Figure. 5. The differences in individual patients ranged from -8.7% to +3.3%. Averaged over all 30 patients, the NTCPs derived from the FPEP algorithm were 1.2% lower than the CCCS, but without statistical significance ( $P = 0.225$ ).

The mean absolute difference between the NTCPs from the two calculation algorithms was 2.1%. The minimum and maximum absolute differences were 0.0% and 8.7%, respectively.

Categorizing the patients' treatments into two dose ranges of 1-14 Gy and 14-50 Gy in terms of the mean dose to CE PRV (as calculated by the CCCS algorithm), the NTCPs from the FPEP algorithm were 0.6% ( $p = 0.860$ ) and 2.6% ( $p = 0.041$ ) lower than CCCS in those low and high dose groups, respectively.

The results of inspecting the effect of the dose calculation algorithms on the predicted CE PRV



NTCPs separately based on tumor site are shown in table 3. The largest difference was 5.5% (oropharynx), although the only statistically significant difference was regarding a 3.1% higher NTCP with CCCS in the nasopharyngeal cases.

Finally, averaged over the six selected patients (one from each tumor site), the differences (FPEP – CCCS) in mean NTCPs obtained for the four published sets of LKB parameters for acute esophagitis were -1.2%, -0.8%, 0.4% and 0.0% for those of Belderbos *et al.* (41), Nijkam *et al.* (40), Zhue *et al.* (31) and Chapet *et al.* (40), respectively. This means that the NTCP difference predicted by the model parameters used in our study was one of the highest among these models.

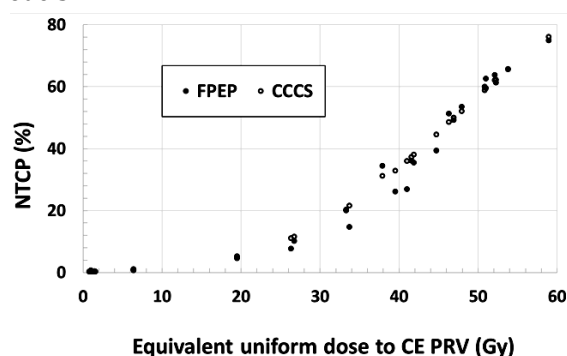


**Figure 2.** The LKB-model predicted relationship between the individual CE PRV NTCPs from the DVH calculated using each algorithm, plotted against the EUD to that structure (as calculated by the CCCS algorithm).

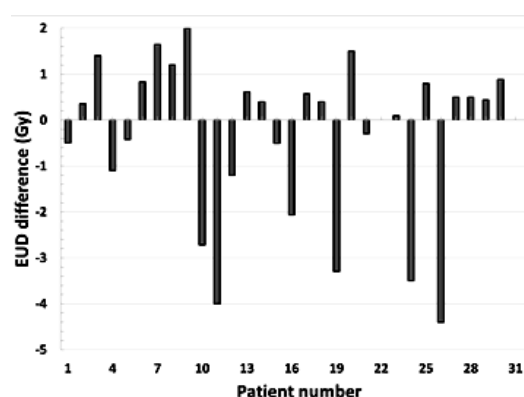


**Figure 3.** The differences between the CE PRV EUDs resulting from the two algorithms (FPEP - CCCS) for all patients.

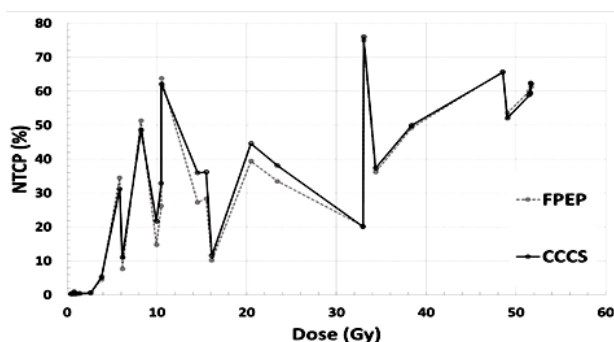


**Figure 4.** The LKB-model predicted relationship between the individual CE PRV NTCPs from the DVHs calculated using each algorithm, plotted against the mean dose to that structure (as calculated by the CCCS algorithm).

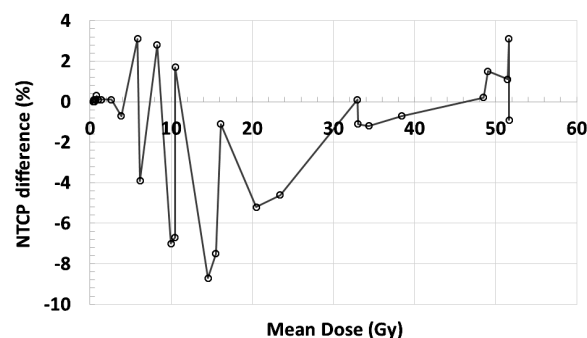


**Figure 5.** The differences between the CE PRV NTCPs from the two algorithms (FPEP - CCCS) plotted against the mean dose.

**Table 3.** The mean ( $\pm$  one standard deviation) CE PRV NTCPs obtained from CCCS and FPEP algorithms for each tumor site (\* denotes  $P < 0.05$ ).

| Tumor site           | Larynx         | Glottis       | Supraglottis   | Oropharynx     | Nasopharynx    | Hypopharynx    |
|----------------------|----------------|---------------|----------------|----------------|----------------|----------------|
| Mean dose (Gy)       | 13.37          | 1.06          | 28.82          | 12.18          | 20.86          | 22.68          |
| Mean NTCP (CCCS) (%) | 35.6 $\pm$ 0.3 | 0.5 $\pm$ 0.0 | 38.9 $\pm$ 0.3 | 30.6 $\pm$ 0.1 | 28.1 $\pm$ 0.1 | 28.1 $\pm$ 0.1 |
| Mean NTCP (FPEP) (%) | 36.5 $\pm$ 0.3 | 0.6 $\pm$ 0.0 | 39.7 $\pm$ 0.3 | 25.1 $\pm$ 0.1 | 25.0 $\pm$ 0.1 | 23.8 $\pm$ 0.0 |
| Difference (%)       | 0.9            | 0.1           | 0.8            | -5.5           | -3.1*          | -4.3           |

## DISCUSSION

In general, the accuracy of dose calculation makes this aspect of the patient workflow one of the strongest links in the so-called RT chain. Accurate determination of dose helps the RT community to establish a more reliable dose-response relationship, about which less is known. In this study, we compared various physical dose and volume statistics produced by the FPEP and CCCS algorithms implemented on the Prowess Panther TPS as typical examples of fairly simple and advanced models, respectively. We did so for the CE PRV as an OAR for acute esophagitis in head-and-neck RT. We then quantified the effects of the differences in the calculated dose on the NTCPs predicted by the LKB model.

One of the main differences between dose calculation algorithms is how they take account of tissue heterogeneities. This issue relates to the heterogeneity of the tissue itself, as well as those of the surrounding media that the primary beam and the scattered photons cross before reaching the tissue. The pattern of secondary electron absorption and scatter is also affected by tissue heterogeneities. Correct modeling of the effects of heterogeneities is of particular importance in the head-and-neck region due to its complex anatomy. We, therefore, included 30 patients that represented several target locations and extents, thereby offering a variety of primary beam trajectories and amounts of secondary radiation reaching the CE PRV.

On average, the more simplistic FPEP algorithm overestimated the mean dose to the CE PRV by a statistically significant 2.0%. The average absolute

difference in mean dose was 2.7% and the maximum difference was 9.3%. The higher values of  $V_{5\text{Gy}}$ ,  $V_{10\text{Gy}}$ ,  $V_{15\text{Gy}}$ ,  $V_{20\text{Gy}}$ ,  $V_{25\text{Gy}}$  and  $V_{30\text{Gy}}$  for FPEP were also statistically significant, while the point-dose and  $D_{2\text{cc}}$  hot spots were similar for both algorithms.

Despite the overestimation of mean dose by the simpler algorithm, the DVH differences led to an underestimation of the LKB-model prediction of the EUD for acute esophagitis by 1.4% (without statistical significance). The mean absolute difference in EUD was 4.5% and the maximum difference was 15.3%. In the 14-50 Gy mean dose range (i.e., the more clinically important higher dose range), the resulting NTCPs with the FPEP algorithm were also underestimated on average by 2.6% compared to the CCCS ( $p = 0.041$ ).

To the best of our knowledge there is no other published paper addressing this issue regarding CE that we can directly compare our results with. We will, therefore, compare and contrast our findings with other somewhat similar studies. As for other OARs in the head and neck and their corresponding endpoints, as an example, in a study done on xerostomia due to the dose to the parotid glands, the mean NTCP calculated by the more advanced Analytical Anisotropic Algorithm (AAA) was lower than the simpler Pencil Beam Convolution (PBC) one <sup>(29)</sup>. Moreover, the NTCP of the lungs as OARs has been shown to be lower than with PBC when modeled based on doses calculated by the CCCS or AAA algorithms <sup>(2, 49)</sup>. These findings differ from our study, where we found the more accurate CCCS algorithm on average led to higher NTCPs. However, there are other published studies in which, at least for some types of cancers (e.g., head and neck and lung), the same pattern has been shown <sup>(29, 50-52)</sup>.

It is well-established that, due to the sigmoidal shape of the EUD-NTCP relationship, the steepness of the high-gradient part of the curve plays a key role in determining the sensitivity of the NTCP to changes in EUD. The steepness of the slope depends on a variety of factors such as the OAR, the endpoint and the level of heterogeneity in the response of individual patients. Of course, a steeper slope means that a small dose change can lead to a large change in NTCP. In this study, we chose the Belderbos *et al.*<sup>(41)</sup> set of parameters of the LKB model in preference over the other published values mainly because it had the largest  $m$  parameter, which determines the slope of the NTCP curve. Consequently, our findings can be considered as a somewhat high estimation of the effect of dose differences on NTCP for the patients and treatment plans included in this study. However, for a fixed NTCP curve, whether the EUD for the OAR of interest in a specific patient plan falls within a shallow or steep part of the curve is expected to have a greater effect <sup>(2)</sup>.

Substantial fluctuations was seen in the relationship between mean CE PRV dose and the

calculated NTCP (figure 4). This is, of course, because the input independent variable for the LKB model is not mean dose but EUD. The corresponding curve versus EUD is a well-behaved sigmoid for the CCCS algorithm (figure 2). The same figure also shows some degree of fluctuation in the FPEP data, due to the fact that the EUD axis was derived from the doses calculated by another algorithm, namely CCCS, and not its own dose calculations, which gave a smooth curve <sup>(32, 43)</sup>.

This study was carried out mainly in the context of 3D conformal treatment planning and the findings apply directly to this type. Additionally, by avoiding the additional complications introduced by small and/or complex segment shapes in IMRT, the findings serve as useful information for isolating the effects of tissue inhomogeneities and contour irregularities in IMRT treatment planning, where the simpler FPEP calculation algorithm is used during optimizations in conjunction with radiobiological quantities such as EUD and NTCP. A further study on the sensitivity of radiobiological indices to the choice of dose calculation algorithm in various types of IMRT treatment planning will be of interest.

## CONCLUSIONS

In the treatment plans of the studied HNC patients, the radiobiological indices of EUD and NTCP for acute esophagitis showed to be only moderately sensitive to the class of dose calculation algorithm employed. On average, the simpler algorithm overestimated the CE PRV mean dose, and somewhat surprisingly, underestimated the LKB-model prediction of the NTCP for acute esophagitis. The underestimation of the NTCP can be of clinical concern, especially as large differences were observed in some patients. Establishing a pattern in terms of which type of algorithm produces higher or lower mean dose or DVH points to a specific OAR in the head and neck is made very difficult by the complexities and multifactorial nature of the problem. Further studies of this type can, therefore, be informative by distinguishing the effects of various shortcomings in the abilities of different algorithms for calculation of dose to specific OARs.

## ACKNOWLEDGEMENTS

*The authors would like to thank the members of the Radio-oncology Department for their help during this study. Provision of a research license from Prowess Inc. is also gratefully acknowledged.*

**Declaration of Conflict of interest:** Declared none.

**Ethical considerations:** Research Ethics Approval ID: IR.SUMS.REC.1398.130.

**Author contributions:** All authors contributed to the

acquisition or analysis of the data, were involved in drafting or revising the manuscript and have approved its final version. MAMS, AS, EF, MM and MA also contributed to the conception or design of the work.

**Financial support:** This article was extracted from parts of postgraduate theses by Ms Arefeh Sheikholeslami and Ms Elahe Fathipour, funded by the Vice-chancellery of Research, Shiraz University of Medical Sciences (project numbers 97-01-10-17432 and 93-01-10, respectively).

## REFERENCES

- Chen W-Z, Xiao Y, Li J (2014) Impact of dose calculation algorithm on radiation therapy. *World Journal of Radiology*, **6**(11): 874.
- Hedin E, Bäck A (2013) Influence of different dose calculation algorithms on the estimate of NTCP for lung complications. *Journal of Applied Clinical Medical Physics*, **14**(5): 127-39.
- Allen Li X, Alber M, Deasy JO, Jackson A, Ken Jee KW, Marks LB, et al. (2012) The use and QA of biologically related models for treatment planning: Short report of the TG-166 of the therapy physics committee of the AAPM. *Medical Physics*, **39**(3): 1386-409.
- The Royal College of Radiologists (2019) The timely delivery of radical radiotherapy: guidelines for the management of unscheduled treatment interruptions, 4th edition. The Royal College of Radiologists, London.
- Brady LW, Perez CA, Wazer DE (2013) Perez & Brady's principles and practice of radiation oncology: Lippincott Williams & Wilkins.
- Van Dyk J, Barnett R, Cygler J, Shragge P (1993) Commissioning and quality assurance of treatment planning computers. *Int J Radiat Oncol Biol Phys*, **26**(2): 261-73.
- Fraass B, Doppke K, Hunt M, Kutcher G, Starkschall G, Stern R, et al. (1998) American association of physicists in medicine radiation therapy committee task group 53: quality assurance for clinical radiotherapy treatment planning. *Medical Physics*, **25**(10): 1773-829.
- Venselaar J, Welleweerd H, Mijneer B (2001) Tolerances for the accuracy of photon beam dose calculations of treatment planning systems. *Radiotherapy and Oncology*, **60**(2): 191-201.
- Bedford J, Childs P, Nordmark Hansen V, Mosleh-Shirazi M, Verhaegen F, Warrington A (2003) Commissioning and quality assurance of the Pinnacle3 radiotherapy treatment planning system for external beam photons. *The British Journal of Radiology*, **76**(903): 163-76.
- Papanikolaou N, Battista J, Boyer A, Kappas C, Klein E, Mackie T (2004) AAPM Report No. 85: tissue inhomogeneity corrections for mega voltage photon beams. American Association of Physicists in Medicine, Madison, WI, USA.
- Chaikh A, Kumar T, Balosso J (2016) What should we know about photon dose calculation algorithms used for radiotherapy? Their impact on dose distribution and medical decisions based on TCP/NTCP. *Int J Cancer Ther Oncol*, **4**(4).
- Fogliata A and Cozzi L (2017) Dose calculation algorithm accuracy for small fields in non-homogeneous media: the lung SBRT case. *Physica Medica*, **44**: 157-62.
- Bahreyni-Toossi MT, Farhood B, Soleymanifard S (2017) Evaluation of dose calculations accuracy of a commercial treatment planning system for the head and neck region in radiotherapy. *Reports of Practical Oncology & Radiotherapy*, **22**(5): 420-7.
- Onizuka R, Araki F, Ohno T, Nakaguchi Y, Kai Y, Tomiyama Y, et al. (2016) Accuracy of dose calculation algorithms for virtual heterogeneous phantoms and intensity-modulated radiation therapy in the head and neck. *Radiological Physics and Technology*, **9**(1): 77-87.
- Mohammadi K, Hassani M, Ghorbani M, Farhood B, Knaup C (2017) Evaluation of the accuracy of various dose calculation algorithms of a commercial treatment planning system in the presence of hip prosthesis and comparison with Monte Carlo. *Journal of Cancer Research and Therapeutics*, **13**(3): 501.
- Dawod T (2015) Evaluation of collapsed cone convolution superposition (CCCS) algorithms in prowl treatment planning system for calculating symmetric and asymmetric field size. *Int J Cancer Ther Oncol*, **3**(2): 8.
- Kim YL, Suh TS, Choe BY, Choi BO, Chung JB, Lee JW, et al. (2016) Dose distribution evaluation of various dose calculation algorithms in inhomogeneous media. *Int J Radiat Res*, **14**(4): 269-78.
- Mosleh-Shirazi MA, Hansen VN, Childs PJ, Warrington AP, Saran FH (2004) Commissioning and implementation of a stereotactic conformal radiotherapy technique using a general-purpose planning system. *Journal of Applied Clinical Medical Physics*, **5**(3): 1-14.
- Zeinali-Rafsanjani B, Mosleh-Shirazi M, Faghihi R, Karbasi S, Mosalaei A (2015) Fast and accurate Monte Carlo modeling of a kilovoltage X-ray therapy unit using a photon-source approximation for treatment planning in complex media. *Journal of Medical Physics/Association of Medical Physicists of India*, **40**(2): 74.
- Mohammadyari P, Faghihi R, Mosleh-Shirazi MA, Lotfi M, Hematiyan MR, Koontz C, et al. (2015) Calculation of dose distribution in compressible breast tissues using finite element modeling, Monte Carlo simulation and thermoluminescence dosimeters. *Physics in Medicine & Biology*, **60**(23): 9185.
- Tahmasebi-Birgani MJ, Mahdavi M, Zabihzadeh M, Lotfi M, Mosleh-Shirazi MA (2018) Simultaneous characterization of electron density and effective atomic number for radiotherapy planning using stoichiometric calibration method and dual energy algorithms. *Australasian Physical & Engineering Sciences in Medicine*, **41**(3): 601-19.
- Zeinali-Rafsanjani B, Faghihi R, Mosleh-Shirazi M, Saeedi-Moghadam M, Jalli R, Sina S (2018) Effect of age-dependent bone electron density on the calculated dose distribution from kilovoltage and megavoltage photon and electron radiotherapy in paediatric MRI-only treatment planning. *The British Journal of Radiology*, **91**(1081): 20170511.
- SM Bentzen (2019) Radiation dose-response relationships. In: Basic clinical radiobiology, 5<sup>th</sup> ed (Michael C. Joiner and Albert J. Van der Kogel, eds.), Taylor & Francis Group, LLC.
- Brink C, Berg M, Nielsen M (2007) Sensitivity of NTCP parameter values against a change of dose calculation algorithm. *Med Phys*, **34**(9): 3579-86.
- Sini C, Broggi S, Fiorino C, Cattaneo GM, Calandrino R (2015) Accuracy of dose calculation algorithms for static and rotational IMRT of lung cancer: A phantom study. *Phys Med*, **31**(4): 382-90.
- Nielsen TB, Wieslander E, Fogliata A, Nielsen M, Hansen O, Brink C (2011) Influence of dose calculation algorithms on the predicted dose distribution and NTCP values for NSCLC patients. *Med Phys*, **38**(5): 2412-8.
- De Jaeger K, Hoogeman MS, Engelsman M, Seppenwoolde Y, Damen EM, Mijneer BJ, et al. (2003) Incorporating an improved dose-calculation algorithm in conformal radiotherapy of lung cancer: re-evaluation of dose in normal lung tissue. *Radiotherapy and Oncology*, **69**(1): 1-10.
- Liang X, Penagaricano J, Zheng D, Morrill S, Zhang X, Corry P, et al. (2016) Radiobiological impact of dose calculation algorithms on biologically optimized IMRT lung stereotactic body radiation therapy plans. *Radiation Oncology*, **11**(1): 10.
- Bufacchi A, Nardiello B, Capparella R, Begnozzi L (2013) Clinical implications in the use of the PBC algorithm versus the AAA by comparison of different NTCP models/parameters. *Radiation Oncology*, **8**(1): 164.
- Chaikh A, Docquière N, Bondiau P-Y, Balosso J (2016) Impact of dose calculation models on radiotherapy outcomes and quality adjusted life years for lung cancer treatment: do we need to measure radiotherapy outcomes to tune the radiobiological parameters of a normal tissue complication probability model? *Translational Lung Cancer Research*, **5**(6): 673.
- Zhu J, Zhang Z-C, Li B-S, Liu M, Yin Y, Yu J-M, et al. (2010) Analysis of acute radiation-induced esophagitis in non-small-cell lung cancer patients using the Lyman NTCP model. *Radiotherapy and Oncology*, **97**(3): 449-54.
- Khan FM, Gibbons JP, Sperduto PW (2016) Khan's Treatment Planning in Radiation Oncology. Lippincott Williams & Wilkins.
- James N, Williams M, Summers E, Jones K, Cottier B (2008) Royal College of Radiologists Clinical Audit S. The management of interruptions to radiotherapy in head and neck cancer: an audit of the effectiveness of national guidelines. *Clin Oncol (R Coll Radiol)*, **20**(8): 599-605.
- Knöös T, Wieslander E, Cozzi L, Brink C, Fogliata A, Albers D, et al. (2006) Comparison of dose calculation algorithms for treatment planning in external photon beam therapy for clinical situations. *Physics in Medicine & Biology*, **51**(22): 5785.
- Christianen ME, Langendijk JA, Westerlaan HE, van de Water TA, Bijl HP (2011) Delineation of organs at risk involved in swallowing

- for radiotherapy treatment planning. *Radiotherapy and Oncology*, **101**(3): 394-402.
36. Prowess Inc. Prowess Panther User Manual. Version 5.4. Concord, CA, USA.
  37. Lyman JT (1985) Complication probability as assessed from dose-volume histograms. *Radiation Research*, **104**(2s): S13-S9.
  38. Kutcher GJ and Burman C (1989) Calculation of complication probability factors for non-uniform normal tissue irradiation: The effective volume method gerald. *Int J Radiat Oncol Biol Phys*, **16**(6): 1623-30.
  39. Uzan J and Nahum A (2012) Radiobiologically guided optimisation of the prescription dose and fractionation scheme in radiotherapy using BioSuite. *The British Journal of Radiology*, **85**(1017): 1279-86.
  40. Nijkamp J, Rossi M, Lebesque J, Belderbos J, van den Heuvel M, Kwant M, *et al.* (2013) Relating acute esophagitis to radiotherapy dose using FDG-PET in concurrent chemo-radiotherapy for locally advanced non-small cell lung cancer. *Radiotherapy and Oncology*, **106**(1): 118-23.
  41. Belderbos J, Heemsbergen W, Hoogeman M, Pengel K, Rossi M, Lebesque J (2005) Acute esophageal toxicity in non-small cell lung cancer patients after high dose conformal radiotherapy. *Radiotherapy and Oncology*, **75**(2): 157-64.
  42. Chapet O, Kong F-M, Lee JS, Hayman JA, Ten Haken RK (2005) Normal tissue complication probability modeling for acute esophagitis in patients treated with conformal radiation therapy for non-small cell lung cancer. *Radiotherapy and Oncology*, **77**(2): 176-81.
  43. Mosleh-Shirazi MA, Amraee A, Mohaghegh F (2019) Dose-response relationship and normal-tissue complication probability of conductive hearing loss in patients undergoing head-and-neck or cranial radiotherapy: A prospective study including 70 ears. *Physica Medica*, **61**: 64-9.
  44. Maguire J, Uzan J, Kelly V (2015) 146: Therapeutic advantage of concurrent chemoradiotherapy with 55 Gy/20 fractions with cisplatin and vinorelbine assessed by comparing control rates predicted by radio-biological (Biosuite) software and clinical results. *Lung Cancer*, **87**: S53.
  45. Senthilkumar K, Das KM, Balasubramanian K, Deka A, Patil B (2016) Estimation of the effects of normal tissue sparing using equivalent uniform dose-based optimization. *Journal of Medical Physics/ Association of Medical Physicists of India*, **41**(2): 123.
  46. Wang L, Bkaer C, Uzan J, Fan J, Jin L, Hayes S, *et al.* (2012) SU-C-  
BRB-04: Isotoxic Hypofractionation for Liver Cancer Radiobiologically Optimized Schedules and Normal Tissue DVH Metrics for NTCP. *Medical Physics*, **39**(6 Part 2): 3601-2.
  47. Wang S, Campbell J, Stenmark MH, Stanton P, Zhao J, Matuszak MM, *et al.* (2018) A model combining age, equivalent uniform dose and IL-8 may predict radiation esophagitis in patients with non-small cell lung cancer. *Radiotherapy and Oncology*, **126**(3): 506-10.
  48. Duijm M, van de Vaart P, Oomen-de Hoop E, Mast ME, Hoogeman MS, Nuytens JJ (2019) Predicting High-Grade Esophagus Toxicity After Treating Central Lung Tumors With Stereotactic Radiation Therapy Using a Normal Tissue Complication Probability Model. *Int J Radiat Oncol Biol Phys*, **106**(1): 73-81.
  49. Petillion S, Swinnen A, Defraene G, Verhoeven K, Weltens C, den Heuvel FV (2014) The photon dose calculation algorithm used in breast radiotherapy has significant impact on the parameters of radiobiological models. *Journal of Applied Clinical Medical Physics*, **15**(4): 259-69.
  50. Chaikh A and Balosso J (2016) NTCP variability in radiotherapy of lung cancer when changing the radiobiologic models and the photon dose calculation algorithms. *J Cancer Clin Oncol*, **2**: 100108.
  51. Miften MM, Beavis AW, Marks LB (2002) Influence of dose calculation model on treatment plan evaluation in conformal radiotherapy: a three-case study. *Medical Dosimetry*, **27**(1): 51-7.
  52. Cattaneo GM, Dell'Oca I, Broggi S, Fiorino C, Perna L, Pasetti M, *et al.* (2008) Treatment planning comparison between conformal radiotherapy and helical tomotherapy in the case of locally advanced-stage NSCLC. *Radiotherapy and Oncology*, **88**(3): 310-8.